THE JOURNAL OF PHYSICAL CHEMISTRY Letters

pubs.acs.org/JPCL

Letter

# Effect of Perovskite Thickness on Electroluminescence and Solar Cell Conversion Efficiency

Monika Rai, Lydia Helena Wong,* and Lioz Etgar*

Cite This: *J. Phys. Chem. Lett.* 2020, 11, 8189–8194

Read Online

ACCESS | Metrics & More | Article Recommendations | Supporting Information

**ABSTRACT:** A hybrid organic–inorganic perovskite in a diode structure can lead to multifunctional device phenomena exhibiting both a high power conversion efficiency (PCE) of a solar cell and strong electroluminescence (EL) efficiency. Nonradiative losses in such multifunctional devices lead to an open circuit voltage ($V_{oc}$) deficit, which is a limiting factor for pushing the efficiency toward the Shockley–Queisser limit. In this work, we analyze and quantify the radiative limit of $V_{oc}$ in a perovskite solar cell as a function of its absorber thickness. We correlate PCE and EL efficiency at varying thicknesses to understand the limiting factors for a high $V_{oc}$. With a certain increase in perovskite thickness, PCE improves but EL efficiency is compromised and vice versa. Thus, correlating these two figures of merit of a solar cell guides the light management strategy together with minimizing nonradiative losses. The results demonstrate that maximizing absorption and emission processes remains paramount for optimizing devices.

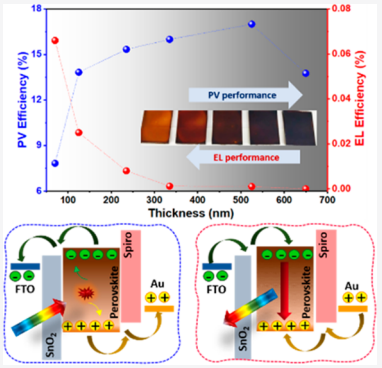




Over the past few years, the performance of lead halide-based perovskite solar cells (PSCs) has revolutionized the photovoltaic field.[1−5] Their strong absorption bands spanning the visible region and excellent charge transport properties together with low-cost solution processability make them ideal candidates for both photovoltaic (PV) devices and light-emitting diodes (LEDs).[6,7] Although the current power conversion efficiency (PCE) of ∼25% is remarkable, the open circuit voltage ($V_{oc}$) of these solar cells remains below their theoretical $V_{oc}$ limit of 1.32 V (corresponding to a 1.6 eV band gap, common for lead halide perovskites) at AM 1.5 G sunlight.[8,9] This loss arises from nonradiative recombination of photogenerated charge carriers, which demands a quantification and identification of the dominating recombination mechanisms.[10] Under a generalized Shockley–Queisser (SQ) approach, Uwe Rau proposed an optoelectronic reciprocity theorem between absorption and emission. Thus, a solar cell that has a theoretical maximum PCE will also give a maximum external quantum efficiency (EQE) of its electroluminescence ($EQE_{EL}$ %) emission.[11] There have been a few reports with high EL efficiency corresponding to high-efficiency devices, but there exists an enormous scope to maximize the emission.[10,12] Moreover, preparing a device that exhibits high PV performance and excellent $EQE_{EL}$ at the same time is a daunting task.[13] However, the key lies in maximizing absorption and emission processes for optimizing high-efficiency devices.

Because of the occurrence of nonradiative losses due to defects, traps, geometrical loss (like reflection, waveguiding, etc.), or other reasons in any real PV system, the $EQE_{EL} < 1$. Therefore, the experimentally observed $V_{oc}$ values of solar cells are lower than the actual radiative limit and are given by[4,13,14]

$$V_{oc}^{cell} = V_{oc}^{rad} - \frac{kT}{q}|\ln\ EQE_{EL}| \quad (1)$$

where $V_{oc}^{cell}$ is the calculated $V_{oc}$ of the solar cell and $V_{oc}^{rad}$ is the radiative limit. This reciprocity relation suggests that a higher $EQE_{EL}$ results in a higher $V_{oc}$. Thus, although the physical mechanism of a solar cell (radiation energy into electricity) and EL (transformation of electrical energy into light) is different, the attainable $V_{oc}$ is related by virtue of eq 1.[13,15] In this work, we use eq 1 to probe the $V_{oc}$ deficit in a $Cs_{0.2}FA_{0.8}Pb(I_{0.85}Br_{0.15})_3$-based PSC by varying the perovskite thickness. The evaluation of $V_{oc}$ from eq 1 was first attempted in a $MAPbI_3$ PSC.[16,17] Whereas for a good PV device, a significant thickness is required to obtain enough light absorption and efficient charge carrier collection, its high $EQE_{EL}$ requires a minimum thickness to reduce waveguiding loss and quenching of EL emission.[18] Importantly, our objective is not to optimize the device structure for the best performance of PSC or EL emission. Instead, we aim to study the correlation between PCE and EL efficiency as a function of absorber thickness. To probe the nonradiative losses in the photoabsorber, we vary only the perovskite thickness, keeping other layers and the deposition technique the same. If a perovskite is sufficiently thick (in the range of its absorption

**Received:** August 2, 2020
**Accepted:** September 4, 2020
**Published:** September 7, 2020

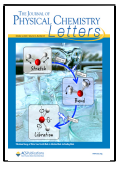







https://dx.doi.org/10.1021/acs.jpclett.0c02363
*J. Phys. Chem. Lett.* 2020, 11, 8189–8194

coefficient),[19] then it leads to an excellent PV performance with enough current density produced. However, EL performance at this thickness is often compromised as photons that are emitted internally are likely to be trapped or reabsorbed (matching emission and absorption energy). This limits the luminescence yield and hence the $V_{oc}$ value. Herein, we fabricate a high-performance MA free perovskite $[Cs_{0.2}FA_{0.8}Pb(I_{0.85}Br_{0.15})_3]$ with a stable and well-studied composition[20,21] for solar cells with a planar structure (n-i-p) using a single-step method and carefully elucidate the effect of its thickness, morphology, and transparency on the PCE and EL performance and illustrate how it defines the inherent losses. These two reciprocal device operations suggest a way to quantify the absorber quality and to minimize defects in the bulk absorber.

Figure 1 illustrates the working mechanism of EL in a LED and PV together with the energy level scheme for a perovskite

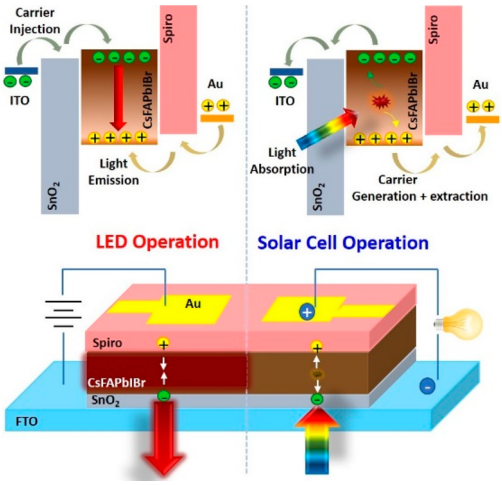


**Figure 1.** Schematic representation of a perovskite LED and solar cell operation with energy level diagrams showing recombination in the LED and carrier extraction in the solar cell.

in an n-i-p structure. In EL, charges are injected through respective charge transport layers (i.e., in a forward bias) into the perovskite where they recombine to give bright near-infrared (NIR) emission. In the PV device, the identical stack is put under 1 sun illumination where electron hole pairs are generated by absorbing light. The generated electrons are extracted by the $SnO_2$ layer electron transport layer (ETL) and hole transport layer (HTL) due to their suitable band matching. The PV device operates in both forward and reverse bias.

Ideally, for the best EL performance, $EQE_{EL} \sim 1$. In that case, from eq 1, we obtain $V_{oc}^{cell} \sim V_{oc}^{rad}$, and hence, we approach the radiative limit of the $V_{oc}$ for a solar cell if the device stack is the same. However, making such a device that is equally good in both operations simultaneously is neither trivial nor straightforward. The perovskite is a defect tolerant material with a low trap density, and most of the radiative recombination happens through a band−band transition.[22,23]

Figure 2a shows the statistical distribution of the PCE at different concentrations of the perovskite solution. The perovskite precursor solution concentration (in molarity) is the direct translation of the absorber thickness as shown in the inset of Figure 2a. The thickness varies from 70 nm for 0.4 M to 630 nm for 1.4 M as deduced from Figure S1, which shows

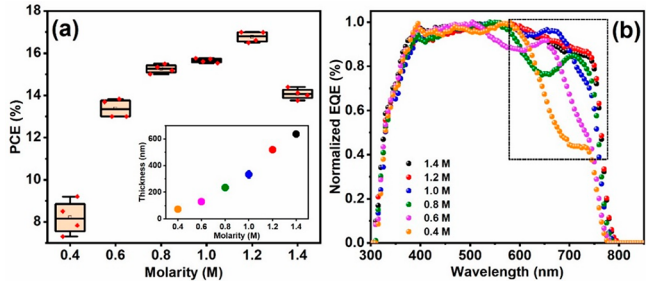


**Figure 2.** (a) Statistical distribution of PV performance of perovskite solar cells at different concentrations. The inset shows the perovskite thickness as a function of concentration. (b) Corresponding EQE spectra.

the SEM (scanning electron microscopy) cross section of a series of devices.

The rest of the PV parameters are shown in Figure S3. There is a continuous increase in $J_{sc}$ with an increase in thickness approaching saturation at 22 mA/cm$^2$ for 1.4 M perovskite. Clearly, the thickness of the absorber is a key parameter for optimal carrier generation. However, crystal quality also plays a significant role in avoiding nonradiative losses of photogenerated carriers due to grain boundaries or other defects in the lattice. The role of a high-quality absorber becomes especially significant at low thicknesses where the level of carrier generation is already low. Figure S2 shows a smaller grain size for a thinner perovskite layer affecting the electrical properties of the material like the generation, transport, and collection of photogenerated carriers. For a thinner perovskite, lesser precursor solution is left for nucleated particles to grow, hence a smaller grain size. With an increasing concentration of perovskite, Ostwald ripening predominates, resulting in large grain growth.

For thicker devices, most of the light harvested by the perovskite contributes to the current. The PCE has a similar trend except that it drops at 1.4 M, as a result of a sudden decrease in $V_{oc}$ and FF due to an overly thick perovskite layer causing aggravated recombination loss.[24] Figure 2b shows the normalized external quantum efficiency ($EQE_{PV}$) of the PV devices showing that the loss in $J_{sc}$ occurs mainly at higher wavelengths (>600 nm). This is expected due to the wavelength-dependent absorption coefficient of perovskite (see Figure S4). The absorption decreases for a thin perovskite, which affects photogeneration especially at longer wavelengths. No significant change in band edge absorption is observed. Thus, we expect the same radiative limit of $V_{oc}$ for all of the devices.

The optical band gap is further calculated from the Tauc plot. Figure S4a shows the ultraviolet−visible absorption spectroscopy of perovskite films on $SnO_2$ substrates showing the signature peak of perovskite at 730−770 nm. The average visible transparency (AVT) decreases with an increase in concentration, which is summarized at the inset of Figure S4a. Whereas a low AVT is required for a high $EQE_{PV}$ as most of the absorbed light contributes to the photogenerated current, one needs a high AVT for $EQE_{EL}$ as it effectively suppresses waveguiding and improves light outcoupling. Due to the high refractive index of the perovskite (≈2.3 near the emission wavelength), waveguiding mode loss is a major loss channel for perovskite and strongly dependent on the thickness of the perovskite layer.[25] Thus, if one is interested in semitransparent PSC specifically for window applications (AVT ∼ 25−35%),


https://dx.doi.org/10.1021/acs.jpclett.0c02363
J. Phys. Chem. Lett. 2020, 11, 8189−8194

these losses are, by default, controlled.[21] With an increase in thickness, therefore, it becomes essential to control it with interfacial texturing to enhance light trapping, which would generate a larger number of charge carriers and hence a higher $J_{sc}$. Figure S4b shows the optical band gap of the perovskite being equal to ∼1.62 eV in agreement with Figure 2b. The X-ray diffraction (XRD) pattern in Figure S5 confirms the cubic phase of the perovskite for different thicknesses.[26]

Next, EL measurement was carried out on the same set of PV devices with different thicknesses by the charge carrier injection method. In the case of the EL mechanism, charge carriers are injected through the respective ETL and HTL layers in forward bias.[27] Panels a−e of Figure 3 show the

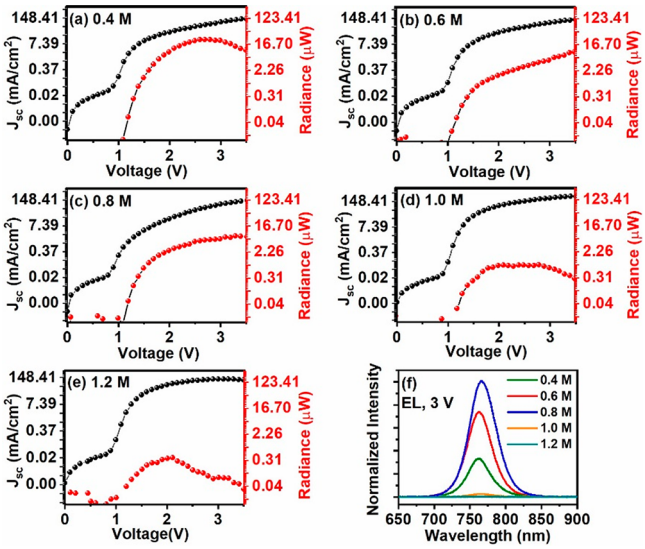


**Figure 3.** (a−e) Current density−voltage ($J$−$V$) (blacks dots) and radiance−voltage (red dots) curves and (f) EL spectra at 3 V applied bias for different concentrations.

current density and EL radiance behavior with respect to the applied voltage. There is no EL performance observed for a 1.4 M film, which can be attributed to the compromised absorber quality and complete quenching. We suspect that joule heating could also be the reason where a thicker perovskite layer forms a stronger barrier for efficient thermal dissipation leading to an elevated junction temperature.[25]

For all of the concentrations, the onset of EL emission is at ∼1 V, which is close to the $V_{oc}$. The plateau region of the EL radiance contracts continuously from 0.4 to 1.2 M with a decrease in its absolute value. This suggests that both EL efficiency and stability decrease as thickness increases. A possible explanation is the large portion of the input power that is converted to heat or self-quenching of EL emission. Also, EL degradation is faster for devices with a thicker perovskite layer, which supports the heat generation/accumulation mechanism. A comparison of the relative intensity of EL spectra is shown in Figure 3f at a constant applied bias of 3 V (which is mostly the plateau region of radiance).

The EL intensity increases from 0.4 to 0.8 M and thereafter decreases. Although we have maximum EL emission for 0.8 M, we do not have a maximum radiance for the same. This is limited by a high level of carrier injection as shown in Figure 4a. EL emission intensity alone does not guarantee a good LED. Therefore, the EL performance is maximum when we have both a low injection current and a high radiative efficiency.

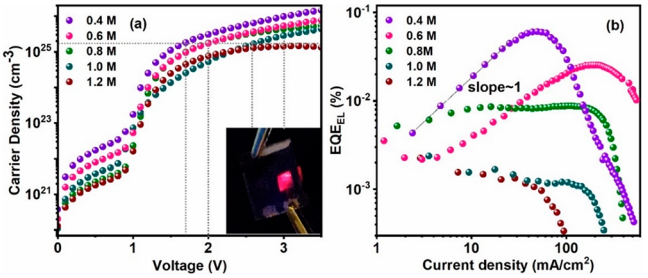


**Figure 4.** (a) Variation of carrier density with applied voltage at different concentrations and thicknesses of perovskite. The inset shows the EL image of the device. (b) EQEs of LED devices plotted as a function of current density for different thicknesses. The black dotted line shows a straight line fit for 0.4 M ($\chi^2$ ∼ 0.999).

To analyze the effect of thickness on film quality, we performed photoluminescence (PL) measurements. The increase in film quality with thickness is corroborated by the improved PL performance (see Figure S6) in terms of a reduced FWHM (full width at half-maximum) and PL maxima shifting to lower wavelengths due to the reduction in grain boundaries (see Figure S2).[28] The time-resolved PL (TRPL) measurements presented in Figure S6d show faster carrier decay for a 1.2 M device than for a 0.4 M device. This can be attributed to various decay channels like bimolecular recombination, trapping, charge extraction, etc., which are subject to investigation (but beyond the scope of this study). For the sake of simplicity, as perovskite is coated on the ETL, which is equivalent to the short circuit condition in PL,[29] the fast decay can arise due to rapid charge carrier transport from the perovskite to the ETL layer. Whereas this sharp decay is beneficial for PV performance in terms of fast extraction of photogenerated carriers, it inhibits the recombination mechanism in EL measurement. Figure S7 further shows the EL and PL spectra plotted together where there is an absolute overlap in the case of 0.4 and 0.6 M but divergence is seen for higher concentrations. The EL maximum remains same, whereas the PL maximum blue shifts. The EL spectra for individual concentrations at a varying applied bias are shown in Figure S8.

Figure 4a shows the variation of carrier density [current density/(elementary charge × thickness)] with voltage for different concentrations. It suggests that the voltage requirement to obtain essentially the same carrier density increases with perovskite thickness (as shown by the vertical gray dotted lines corresponding to a carrier density of $2 \times 10^{25}$ $cm^{-3}$). For a good EL emission, the carrier injection should happen at the minimum applied bias. The bias increases with absorber thickness as the spatial distribution of injected carriers offers resistance to recombination.[30,31]

Figure 4b shows the $EQE_{EL}$ with respect to the injected current density for devices with different concentrations. By plotting $\ln(EQE_{EL})$ as a function of $\ln J_{inj}$ (injection current), we can determine the ideality factor ($n$) of the device.[32] If we compare


https://dx.doi.org/10.1021/acs.jpclett.0c02363
J. Phys. Chem. Lett. 2020, 11, 8189−8194

Table 1. Concentrations and Device Parameters $J_{sc}$ and $V_{oc}$, Calculated $J_o$, $EQE_{EL}$, Calculated $J_o^{rad}$, Calculated $V_o^{rad}$, Calculated $V_o^{non\text{-}rad}$, and Calculated $V_{oc}^{cell}$

| concentration (M) | $J_{sc}$ (mA/cm$^2$) | $V_{oc}$ (V) | $J_o$ (mA/cm$^2$) | $EQE_{EL}$ (%) | $J_o^{rad}$ (mA/cm$^2$) | $V_{oc}^{rad}$ (V) | $V_{oc}^{non\text{-}rad}$ (V) | $V_{oc}^{cell}$ (V) |
|---|---|---|---|---|---|---|---|---|
| 1.2 | 21.6 | 1.03 | $1.09 \times 10^{-16}$ | 0.001 | $1.09 \times 10^{-19}$ | 1.209 | 0.178 | 1.031 |
| 1.0 | 21 | 1.04 | $7.18 \times 10^{-17}$ | 0.002 | $1.44 \times 10^{-19}$ | 1.201 | 0.16 | 1.041 |
| 0.8 | 20 | 1.04 | $6.84 \times 10^{-17}$ | 0.007 | $4.79 \times 10^{-19}$ | 1.170 | 0.128 | 1.040 |
| 0.6 | 17.5 | 1.09 | $8.66 \times 10^{-18}$ | 0.008 | $6.93 \times 10^{-20}$ | 1.215 | 0.125 | 1.089 |
| 0.4 | 12 | 1.09 | $5.94 \times 10^{-18}$ | 0.04 | $2.38 \times 10^{-19}$ | 1.173 | 0.083 | 1.090 |

$$V_{oc}^{cal} = \frac{kT}{q}\ln\left(\frac{J_{sc}}{J_o^{rad}}\right) - \frac{kT}{q}\ln(EQE_{EL}) = n\frac{kT}{q}\ln\left(\frac{J_{sc}}{J_o}\right) \quad (2)$$

where $n$ is the ideality factor and $EQE_{EL}$ a function of injection current, we see that when $n = 1$, the $EQE_{EL}$ should be constant, whereas it should increase linearly with injection current when $n = 2$.[33] For a 0.4 M device, the slope is 1; i.e., $EQE_{EL}$ increases linearly with injection current, indicating that much of the recombination happens through defects/trap-assisted nonradiative recombination [Shockley−Read−Hall (SRH)]. Thus, the occurrence of SRH recombination suggests that $n = 2$, and for low-thickness absorbers, it can be attributed to shallow or surface defects originating from the low surface:volume ratio of the grains (see Figure S2).[34,35] With an increase in thickness, $EQE_{EL}$ becomes constant, i.e., $n \approx 1$, implying band-to-band recombination. Thus, whereas the EL is strong and stable in thin absorbers, it has nonradiative decay channels due to grain boundary defects. As the thickness increases to optimum values, EL performance declines, but most of the recombination is radiative, suggesting a smaller number of defects. These counter behaviors largely affect the photovoltage values, and therefore, maximizing the $EQE_{EL}$ is the key. Table 1 shows the values of $V_{oc}$, $J_{sc}$, and $EQE_{EL}$ values for each concentration where the injection current equals the photocurrent ($J_{sc}$, measured at 1 sun). The value of the dark current ($J_o$) is calculated using the equation[17]

$$J_o = \frac{J_{sc}}{\exp\left(\frac{V_{oc}}{kT/q}\right)} \quad (3)$$

Followed by calculating the dark saturation current ($J_o^{rad}$) in the radiative limit:

$$J_o^{rad} = J_o EQE_{EL} \quad (4)$$

Finally, $V_{oc}^{rad}$ and $V_{oc}^{non\text{-}rad}$ are calculated using

$$V_{oc}^{rad} = \frac{kT}{q}\ln\left(\frac{J_{sc}}{J_o^{rad}}\right),\ V_{oc}^{non\text{-}rad} = \frac{kT}{q}\ln|EQE_{EL}| \quad (5)$$

At last, using eq 1, the calculated $V_{oc}$ ($V_{oc}^{cell} = V_{oc}^{rad} - V_{oc}^{non\text{-}rad}$) is derived.

We now see that $V_{oc}^{rad} \sim 1.2$ V for our device and the calculated $V_{oc}$ matches the measured $V_{oc}$. Although $V_{oc}^{rad}$ is lower in our case than values reported in the literature,[17] being a device property, it relies on how well the device is made and how well measurements are performed. Clearly, $V_{oc}^{cell}$ is closer to the radiative limit for thinner devices.

Figure 5 shows the link between the PV and the EL performance as suggested by eq 1. Figure 5a shows that the $V_{oc}$ deficit ($\Delta V_{oc} = V_{oc}^{non\text{-}rad}$) increases with concentration. In other words, it is a measure of nonradiative losses leading to the $V_{oc}$ deficit that shows an increment with thickness. In Figure 5b, the PV performance improves whereas EL performance decreases within a range of increasing concentrations. The major improvement in PCE comes from the current density, which is primarily a function of the absorber thickness, whereas $EQE_{EL}$ improves if we have a sufficiently thin absorber to overcome luminescence quenching. Absorber thickness is one common factor that collectively affects these two functionalities.

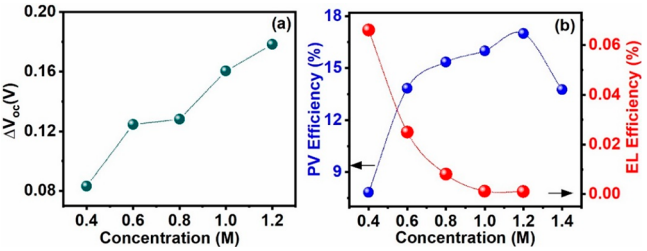


Figure 5. (a) $V_{oc}$ deficit ($\Delta V_{oc}$) as a function of concentration. (b) Comparison of PV and LED efficiency with the concentration of the perovskite layer.

In conclusion, we used the same n-i-p device stack to study the PV and the EL behavior. To do that, we vary the perovskite thickness and follow the $V_{oc}$ deficit that determines the overall efficiency. Moreover, we analyzed the loss of the experimental $V_{oc}$ measured from the PV as compared to the $V_{oc}$ estimated from the EL. Clearly, thickness brings in major loss mechanisms, which decreases $EQE_{EL}$. SRH recombination and insufficient photogeneration of carriers limit the PV performance of the thinner device. For the thicker device, the high carrier injection requirement to obtain EL limits device stability and accelerates degradation pathways. We conclude that to maximize PCE and EL efficiency, one must maximize absorptance and emittance. This can be done by quantifying the achievable $V_{oc}$ and improving the absorber accordingly. In the case of thin PSCs that show strong EL but poor current density, a photon management/concentration strategy can be adopted to overcome carrier limitation. Nonradiative recombination can be mitigated via the passivation of defects, particularly at grain boundaries and interfaces. For standard thicknesses with a high PV efficiency but a compromised EL, device texturing can be beneficial to limit the optical losses.

## ■ ASSOCIATED CONTENT

### Supporting Information

The Supporting Information is available free of charge at https://pubs.acs.org/doi/10.1021/acs.jpclett.0c02363.

Experimental procedure for device fabrication and details of characterizations, SEM images, device performance, transmittance data, XRD measurements, and PL, TRPL, and EL measurements (PDF)



https://dx.doi.org/10.1021/acs.jpclett.0c02363
J. Phys. Chem. Lett. 2020, 11, 8189−8194

## AUTHOR INFORMATION


### Corresponding Authors

**Lioz Etgar** − *Campus for Research Excellence and Technological Enterprise (CREATE), Singapore 138602; The Hebrew University of Jerusalem, Institute of Chemistry, Casali Center for Applied Chemistry, Jerusalem 91904, Israel;* orcid.org/0000-0001-6158-8520; Email: lioz.etgar@mail.huji.ac.il

**Lydia Helena Wong** − *Campus for Research Excellence and Technological Enterprise (CREATE), Singapore 138602; School of Material Science and Engineering, Nanyang Technological University, Singapore 639798;* orcid.org/0000-0001-9059-1745; Email: LydiaWong@ntu.edu.sg

### Author

**Monika Rai** − *Campus for Research Excellence and Technological Enterprise (CREATE), Singapore 138602; School of Material Science and Engineering, Nanyang Technological University, Singapore 639798*

Complete contact information is available at: https://pubs.acs.org/10.1021/acs.jpclett.0c02363


### Author Contributions

L.E. and M.R. conceived and planned the work. M.R. executed the experiments and wrote the first version of the manuscript. L.H.W. and L.E. finalized the manuscript.

### Notes

The authors declare no competing financial interest.

## ACKNOWLEDGMENTS

This research is supported by the National Research Foundation, Prime Minister's Office, Singapore under its Campus for Research Excellence and Technological Enterprise (CREATE) programme.

## REFERENCES


(1) Pazos-Outón, L. M.; Xiao, T. P.; Yablonovitch, E. Fundamental Efficiency Limit of Lead Iodide Perovskite Solar Cells. *J. Phys. Chem. Lett.* **2018**, *9* (7), 1703−1711.

(2) Gao, P.; Grätzel, M.; Nazeeruddin, M. K. Organohalide Lead Perovskites for Photovoltaic Applications. *Energy Environ. Sci.* **2014**, *7* (8), 2448−2463.

(3) Snaith, H. J. Perovskites: The Emergence of a New Era for Low-Cost, High-Efficiency Solar Cells. *J. Phys. Chem. Lett.* **2013**, *4* (21), 3623−3630.

(4) Nayak, P. K.; Mahesh, S.; Snaith, H. J.; Cahen, D. Photovoltaic Solar Cell Technologies: Analysing The State of The Art. *Nat. Rev. Mater.* **2019**, *4* (4), 269−285.

(5) Park, N.-G. Organometal Perovskite Light Absorbers Toward a 20% Efficiency Low-Cost Solid-State Mesoscopic Solar Cell. *J. Phys. Chem. Lett.* **2013**, *4* (15), 2423−2429.

(6) Quan, L. N.; García de Arquer, F. P.; Sabatini, R. P.; Sargent, E. H. Perovskites for Light Emission. *Adv. Mater.* **2018**, *30* (45), 1801996.

(7) Sum, T. C.; Mathews, N. Advancements in Perovskite Solar Cells: Photophysics Behind The Photovoltaics. *Energy Environ. Sci.* **2014**, *7* (8), 2518−2534.

(8) National Renewable Energy Laboratory. Best Research-Cell Efficiency Chart. https://www.nrel.gov/pv/cell-efficiency.html. 2020.

(9) Rühle, S. Tabulated Values of The Shockley−Queisser Limit for Single Junction Solar Cells. *Sol. Energy* **2016**, *130*, 139−147.

(10) Bi, D.; Tress, W.; Dar, M. I.; Gao, P.; Luo, J.; Renevier, C.; Schenk, K.; Abate, A.; Giordano, F.; Correa Baena, J.-P.; et al. Efficient Luminescent Solar Cells Based on Tailored Mixed-Cation Perovskites. *Sci. Adv.* **2016**, *2* (1), No. e1501170.

(11) Rau, U. Reciprocity Relation Between Photovoltaic Quantum Efficiency and Electroluminescent Emission of Solar Cells. *Phys. Rev. B: Condens. Matter Mater. Phys.* **2007**, *76* (8), 085303.

(12) Tavakoli, M. M.; Tress, W.; Milić, J. V.; Kubicki, D.; Emsley, L.; Grätzel, M. Addition of Adamantylammonium Iodide to Hole Transport Layers Enables Highly Efficient and Electroluminescent Perovskite Solar Cells. *Energy Environ. Sci.* **2018**, *11* (11), 3310−3320.

(13) Yablonovitch, E.; Miller, O. D.; Kurtz, S. R. A Great Solar Cell Also Needs to be A Great LED: External Fluorescence Leads to New Efficiency Record. *AIP Conf. Proc.* **2012**, *1519* (1), 9−11.

(14) Ross, R. T. Some Thermodynamics of Photochemical Systems. *J. Chem. Phys.* **1967**, *46* (12), 4590−4593.

(15) Green, M. Radiative Efficiency of State-Of-The-Art Photovoltaic Cells. *Prog. Photovoltaics* **2012**, *20*, 472−476.

(16) Tress, W.; Marinova, N.; Inganäs, O.; Nazeeruddin, M. K.; Zakeeruddin, S. M.; Graetzel, M. Predicting the Open-Circuit Voltage of $CH_3NH_3PbI_3$ Perovskite Solar Cells Using Electroluminescence and Photovoltaic Quantum Efficiency Spectra: The Role of Radiative and Non-Radiative Recombination. *Adv. Energy Mater.* **2015**, *5* (3), 1400812.

(17) Tvingstedt, K.; Malinkiewicz, O.; Baumann, A.; Deibel, C.; Snaith, H. J.; Dyakonov, V.; Bolink, H. J. Radiative Efficiency of Lead Iodide Based Perovskite Solar Cells. *Sci. Rep.* **2015**, *4* (1), 6071.

(18) Liu, D.; Gangishetty, M. K.; Kelly, T. L. Effect Of $CH_3NH_3PbI_3$ Thickness on Device Efficiency in Planar Heterojunction Perovskite Solar Cells. *J. Mater. Chem. A* **2014**, *2* (46), 19873−19881.

(19) Stranks, S. D.; Eperon, G. E.; Grancini, G.; Menelaou, C.; Alcocer, M. J.; Leijtens, T.; Herz, L. M.; Petrozza, A.; Snaith, H. J. Electron-Hole Diffusion Lengths Exceeding 1 Micrometer in an Organometal Trihalide Perovskite Absorber. *Science* **2013**, *342* (6156), 341−344.

(20) Rehman, W.; McMeekin, D. P.; Patel, J. B.; Milot, R. L.; Johnston, M. B.; Snaith, H. J.; Herz, L. M. Photovoltaic Mixed-Cation Lead Mixed-Halide Perovskites: Links Between Crystallinity, Photo-Stability And Electronic Properties. *Energy Environ. Sci.* **2017**, *10* (1), 361−369.

(21) Rai, M.; Rahmany, S.; Lim, S. S.; Magdassi, S.; Wong, L. H.; Etgar, L. Hot Dipping Post Treatment for Improved Efficiency in Micro Patterned Semi-Transparent Perovskite Solar Cells. *J. Mater. Chem. A* **2018**, *6* (46), 23787−23796.

(22) Steirer, K.; Schulz, P.; Teeter, G.; Stevanovic, V.; Yang, M.; Zhu, K.; Berry, J. Defect Tolerance in Methylammonium Lead Triiodide Perovskite. *ACS Energy Lett.* **2016**, *1* (2), 360−366.

(23) Meggiolaro, D.; Motti, S. G.; Mosconi, E.; Barker, A. J.; Ball, J.; Andrea Riccardo Perini, C.; Deschler, F.; Petrozza, A.; De Angelis, F. Iodine Chemistry Determines The Defect Tolerance of Lead-Halide Perovskites. *Energy Environ. Sci.* **2018**, *11* (3), 702−713.

(24) Chen, B.-X.; Rao, H.-S.; Chen, H.-Y.; Li, W.-G.; Kuang, D.-B.; Su, C.-Y. Ordered Macroporous $CH_3NH_3PbI_3$ Perovskite Semi-transparent Film for High-Performance Solar Cells. *J. Mater. Chem. A* **2016**, *4* (40), 15662−15669.

(25) Zhao, L.; Lee, K. M.; Roh, K.; Khan, S. U. Z.; Rand, B. P. Improved Outcoupling Efficiency and Stability of Perovskite Light-Emitting Diodes using Thin Emitting Layers. *Adv. Mater.* **2019**, *31* (2), 1805836.

(26) Prathapani, S.; Bhargava, P.; Mallick, S. Electronic Band Structure and Carrier Concentration of Formamidinium−Cesium Mixed Cation Lead Mixed Halide Hybrid Perovskites. *Appl. Phys. Lett.* **2018**, *112* (9), 092104.

(27) Piper, W. W.; Williams, F. E. Theory of Electroluminescence. *Phys. Rev.* **1955**, *98* (6), 1809−1813.

(28) Watthage, S. C.; Song, Z.; Shrestha, N.; Phillips, A. B.; Liyanage, G. K.; Roland, P. J.; Ellingson, R. J.; Heben, M. J. Enhanced Grain Size, Photoluminescence, and Photoconversion Efficiency with Cadmium Addition during the Two-Step Growth of $CH_3NH_3PbI_3$. *ACS Appl. Mater. Interfaces* **2017**, *9* (3), 2334−2341.

(29) Kirchartz, T.; Márquez, J. A.; Stolterfoht, M.; Unold, T. Photoluminescence-Based Characterization of Halide Perovskites for Photovoltaics. *Adv. Energy Mater.* **2020**, *10* (26), 1904134.

(30) Gegevičius, R.; Franckevičius, M.; Chmeliov, J.; Tress, W.; Gulbinas, V. Electroluminescence Dynamics in Perovskite Solar Cells Reveals Giant Overshoot Effect. *J. Phys. Chem. Lett.* **2019**, *10* (8), 1779−1783.
(31) Jaramillo-Quintero, O. A.; Sanchez, R. S.; Rincon, M.; Mora-Sero, I. Bright Visible-Infrared Light Emitting Diodes Based on Hybrid Halide Perovskite with Spiro-OMeTAD as a Hole-Injecting Layer. *J. Phys. Chem. Lett.* **2015**, *6* (10), 1883−1890.
(32) Tress, W.; Yavari, M.; Domanski, K.; Yadav, P.; Niesen, B.; Correa Baena, J. P.; Hagfeldt, A.; Graetzel, M. Interpretation and Evolution of Open-Circuit Voltage, Recombination, Ideality Factor and Subgap Defect States during Reversible Light-Soaking and Irreversible Degradation of Perovskite Solar Cells. *Energy Environ. Sci.* **2018**, *11* (1), 151−165.
(33) Marinova, N.; Tress, W.; Humphry-Baker, R.; Dar, M. I.; Bojinov, V.; Zakeeruddin, S. M.; Nazeeruddin, M. K.; Grätzel, M. Light Harvesting and Charge Recombination in $CH_3NH_3PbI_3$ Perovskite Solar Cells Studied by Hole Transport Layer Thickness Variation. *ACS Nano* **2015**, *9* (4), 4200−4209.
(34) Calado, P.; Burkitt, D.; Yao, J.; Troughton, J.; Watson, T. M.; Carnie, M. J.; Telford, A. M.; O'Regan, B. C.; Nelson, J.; Barnes, P. R. F. Identifying Dominant Recombination Mechanisms in Perovskite Solar Cells by Measuring the Transient Ideality Factor. *Phys. Rev. Appl.* **2019**, *11* (4), 044005.
(35) Jiang, Q.; Zhao, Y.; Zhang, X.; Yang, X.; Chen, Y.; Chu, Z.; Ye, Q.; Li, X.; Yin, Z.; You, J. Surface Passivation of Perovskite Film for Efficient Solar Cells. *Nat. Photonics* **2019**, *13* (7), 460−466.


https://dx.doi.org/10.1021/acs.jpclett.0c02363
*J. Phys. Chem. Lett.* 2020, 11, 8189−8194